Polarization-mode dispersion of a circulating loop

T. I. Lakoba

Department of Mathematics, University of Central Florida, Orlando, Florida 32816

C. Dorrer

Bell Laboratories, Lucent Technologies, 101 Crawfords Corner Road, Holmdel, New Jersey 07733

D. N. Maywar*

Laboratory for Laser Energetics, University of Rochester, 250 East River Road, Rochester, New York 14623

Received March 10, 2003; revised manuscript received September 5, 2003; accepted September 29, 2003

We derive an analytic expression for the evolution of the differential group delay (DGD) in a fiber-optic circulating loop. We distill a simple analytic solution for the *average* DGD and show that it accumulates approximately linearly with transmission distance. The scaling of this linear function is confirmed experimentally using a long-haul fiber-optic transmission test-bed. This result is contrasted with DGD accumulation in a long straight-line transmission system, where the average DGD accumulates as a square root of the system's length. © 2004 Optical Society of America

OCIS codes: 060.2300, 060.2330, 060.2360, 060.5530.

1. INTRODUCTION

Polarization-mode dispersion (PMD) is one of the main factors limiting fiber-optic transmission at 40 Gb/s over distances of a thousand kilometers and longer. First-order PMD splits the pulse into two orthogonally polarized components that are delayed relative to each other.[1] The differential group delay (DGD) between these components can often be directly related to the transmission penalty occurring due to PMD.[2] Moreover, the mean DGD uniquely determines the statistics of all orders of PMD.[3–6] In an actual transmission link of length L, the mean DGD is known to grow as $\sqrt{L}$ and have a Maxwellian probability distribution.

However, the main tool of testing transmission performance in a laboratory is a circulating loop (CL), where the signal passes through the same loop of fiber several times before being detected. In most instances, CL system tests are performed without polarization scrambling from one loop passage to the next, and hence the polarization state of the signal undergoes the same transformation after each passage. For this situation, numerical simulations showed[7] nearly linear dependence of the mean DGD on the number of passages over the CL (or, equivalently, on the total transmission distance). To emulate a straight-line system by restoring a square-root dependence of the average DGD on the propagation distance, the authors of Ref. 7 proposed to scramble the polarization of the signal at the beginning of each circulation. Reference 8 reports experimental measurements suggesting that the PMD affects the bit error rate (BER) of a CL-based transmission system much stronger than it would in a straight-line system. Experimental results reported in Ref. 8 also show that scrambling the signal's polarization after each circulation restores the bit-error-rate probability distribution to that expected for a straight-line system.

In Section 2 of this paper, we use the Jones matrix approach to derive analytical expressions for both a particular realization and the mean value of the DGD of a CL without polarization scrambling and confirm that, for more than four or five passages around the loop, the mean DGD scales almost linearly with distance. We carry out the analysis without taking into account possible polarization-dependent loss of the CL, assuming that it is sufficiently small.

In Section 3, we present results of experimental measurements of PMD of a CL, which confirm the above theoretical derivation. Although many different techniques exist to quantitatively assess PMD in a device,[9] most of them cannot be efficiently used in a CL. Techniques based on the propagation of a broadband source signal in the device under test, or the wide tuning of a cw source, are compromised by spectral shaping either outside the loop (for example, by a multiplexer and demultiplexer) or inside the loop (by the spectral dependence of the gain of the amplifiers and the gain-equalization filters). Therefore the DGD in a CL must be obtained from a spectrally narrow-band measurement. Also, when one considers the photons at the output of the loop, different instants in time correspond to different number of circulations in the loop. Therefore any measurement technique must temporally resolve the signal at the output of the loop. In addition, the measurement of DGD must be performed faster than the time for significant changes of the polarization state of the system under test. The approach that we used and that we describe in detail in Section 3 meets

all of the aforementioned requirements. We also experimentally confirm both the almost linear and square-root dependences of the average DGD on the number of circulations for the respective cases where the signal's polarization is not, and is, scrambled after each circulation around the loop.

In Section 4, we provide an intuitive explanation of the almost linear dependence of the average DGD on the number of circulations in a loop without polarization scrambling. We also point to an implication that our results have for the statistics of higher orders of PMD in a CL.

2. THEORY

Let the two-component electric field vector $\mathbf{E}_{\text{in}}(\omega)$ be a continuous-wave input to the CL, and $\mathbf{E}_{\text{out}}(\omega)$ be the output after one passage around the loop. Then $\mathbf{E}_{\text{out}}(\omega) = T(\omega)\mathbf{E}_{\text{in}}(\omega)$, where $T(\omega)$ is the loop's frequency-dependent transfer matrix. (Below we omit the explicit dependence of quantities on ω.) Since we ignore polarization-dependent loss, T is a unitary matrix, i.e., $T^+ = T^{-1}$, where the superscript + stands for Hermitian conjugation. As was shown in the original work by Poole and Wagner,[1] the eigenvalue problem

$$[T^{-1}T' - i\tau_1]\mathbf{e}_1 = 0 \tag{1}$$

determines the polarization of, and a DGD between, the two components into which an input pulse is split by PMD. Namely, the two eigenvectors, $\mathbf{e}_{1+}$ and $\mathbf{e}_{1-}$, determine the polarization of those components, while the difference between their eigenvalues, $(\tau_{1+} - \tau_{1-})$, equals the DGD. In Eq. (1), $T' \equiv \mathrm{d}T/\mathrm{d}\omega$, and we use the subscript "1" to denote quantities pertaining to *one* passage around the CL. One can show that the eigenvectors $\mathbf{e}_{1\pm}$ of Eq. (1), referred to as principal states of polarization, are orthogonal, and $\tau_{1+} = -\tau_{1-} \equiv \tau_1$.[1] We refer to the matrix $T^{-1}T'$ as the PMD matrix of (one circulation about) the loop.

Our goal is to find the DGD after N passages around the CL, i.e., $2\tau_N \equiv (\tau_{N+} - \tau_{N-})$, where $\tau_{N\pm}$ are the eigenvalues of

$$[(T^N)^{-1}(T^N)' - i\tau_N]\mathbf{e}_N = 0. \tag{2}$$

Equation (2) can be rewritten as

$$[(T^{-(N-1)}(T^{-1}T')T^{N-1} + T^{-(N-2)}(T^{-1}T')T^{N-2} + \cdots + T^{-1}T') - i\tau_N]\mathbf{e}_N = 0. \tag{3}$$

Each term of the form $T^{-k}(T^{-1}T')T^k$ in Eq. (3) has eigenvectors $\mathbf{v}_{k\pm} = T^{-k}\mathbf{e}_{1\pm}$, whence one can deduce that that term represents a contribution of the kth passage around the loop to the total PMD matrix $(T^N)^{-1}(T^N)'$. In order to compute this contribution, one needs to know how the rotation matrix T transforms the principal states of polarization $\mathbf{e}_{1\pm}$. To this end, we first introduce eigenvectors of T that satisfy $T\mathbf{t}_\pm = \lambda_\pm\mathbf{t}_\pm$. The most general form of the unitary matrix T is

$$T = \begin{bmatrix} \cos\varphi\exp(i\theta_1) & -\sin\varphi\exp(i\theta_2) \\ \sin\varphi\exp(-i\theta_2) & \cos\varphi\exp(-i\theta_1) \end{bmatrix}, \tag{4}$$

with its eigenvalues being $\lambda_\pm = \cos\theta_1\cos\varphi \pm i\sqrt{1 - \cos^2\theta_1\cos^2\varphi}$. One can show by direct calculation that $\mathbf{t}_+$ and $\mathbf{t}_-$ are orthogonal: $\mathbf{t}_+^* \cdot \mathbf{t}_- = 0$. Thus we have two sets of orthogonal pairs of vectors: $\mathbf{e}_\pm$ and $\mathbf{t}_\pm$, of which the former are the principal states of polarization and the latter are the eigenvectors, of the CL. They can be related by a unitary transformation Φ:

$$(\mathbf{e}_{1+}, \mathbf{e}_{1-}) = (\mathbf{t}_+, \mathbf{t}_-)\Phi, \tag{5a}$$

$$(\mathbf{t}_+, \mathbf{t}_-) = (\mathbf{e}_{1+}, \mathbf{e}_{1-})\Phi^+. \tag{5b}$$

Since Φ is unitary, it can be written in a form similar to T:

$$\Phi = \begin{bmatrix} \cos\xi\exp(i\psi_1) & -\sin\xi\exp(i\psi_2) \\ \sin\xi\exp(-i\psi_2) & \cos\xi\exp(-i\psi_1) \end{bmatrix}. \tag{6}$$

It is an easy matter to show that (2ξ) equals the angle between the PMD vector and the loop eigenvector on the Poincaré sphere.

We now expand the input field as $\mathbf{E}_{\text{in}} = \mathcal{E}_+\mathbf{t}_+ + \mathcal{E}_-\mathbf{t}_-$, where $\mathcal{E}_\pm$ are the expansion coefficients. Substituting this equation into Eq. (3) and using the definition of $\mathbf{t}_\pm$, one finds

$$\mathcal{E}_+[(T^{-(N-1)}(T^{-1}T')\lambda_+^{N-1} + T^{-(N-2)}(T^{-1}T')\lambda_+^{N-2} + \cdots + T^{-1}T')]\mathbf{t}_+ + \mathcal{E}_-[(T^{-(N-1)}(T^{-1}T')\lambda_-^{N-1} + T^{-(N-2)}(T^{-1}T')\lambda_-^{N-2} + \cdots + T^{-1}T')]\mathbf{t}_- = i\tau_N(\mathcal{E}_+\mathbf{t}_+ + \mathcal{E}_-\mathbf{t}_-). \tag{7}$$

Now, in each term on the left-hand side of Eq. (7), there is a product of the form $T^{-m}(T^{-1}T')$, with $0 \leqslant m \leqslant N - 1$, acting on $\mathbf{t}_\pm$. Therefore it is convenient to use Eq. (5b) to expand $\mathbf{t}_\pm$ over the basis of the matrix $T^{-1}T'$ [see Eq. (1)] and then use the inverse relation, Eq. (5a), to switch back to the basis of the matrix T^{-m}. Implementing these steps and using Eq. (6), we find

$$i\tau_1\left[\mathcal{E}_+N\cos 2\xi + \mathcal{E}_-\frac{1 - \exp(i\Lambda N)}{1 - \exp(i\Lambda)} \times \exp(i\psi)\sin 2\xi\right]\mathbf{t}_+ - i\tau_1\left[\mathcal{E}_-N\cos 2\xi - \mathcal{E}_+\left(\frac{1 - \exp(i\Lambda N)}{1 - \exp(i\Lambda)}\exp(i\psi)\right)^*\sin 2\xi\right]\mathbf{t}_- = i\tau_N(\mathcal{E}_+\mathbf{t}_+ + \mathcal{E}_-\mathbf{t}_-), \tag{8}$$

where $\exp(i\Lambda) \equiv \lambda_-/\lambda_+$ (or, equivalently, $\cos\Lambda/2 = \cos\theta_1\cos\varphi$) and $\psi = \psi_1 + \psi_2$. Equation (8) yields a system of two scalar homogeneous equations on the coefficients $\mathcal{E}_\pm$, from which both their ratio and the eigenvalue τ_N can be determined. For the latter, we find

$$\tau_N^2 = \tau_1^2\left[N^2\cos^2 2\xi + \sin^2 2\xi\frac{\sin^2(N\Lambda/2)}{\sin^2(\Lambda/2)}\right]. \tag{9}$$

Equation (9) determines a relation between the DGDs, $2\tau_N$ and $2\tau_1$, of N passages and a single passage around the CL for a *particular realization* of the loop's transfer matrix T. We note that the same result could also be obtained using the PMD concatenation rule of Ref. 10. That reference uses the Muller matrix representation for

rotation of (real-valued, three-component) Stokes vectors on the Poincaré sphere, whereas our analysis uses Jones matrices to represent rotations in the space of complex-valued, two-component vectors of polarized electric fields.

We now proceed to calculation of the average of the right-hand side of Eq. (9). It contains three random quantities: τ_1, ξ, and Λ. Recall that Λ depends only on the transfer matrix T, while τ_1 and ξ, characterizing the magnitude and direction of the loop's PMD vector, depend on $T^{-1}T'$. Therefore τ_1 are ξ are statistically independent of Λ, because T', and hence the product $T^{-1}T'$, are independent of T itself. Furthermore, although the magnitude and direction of the PMD vector are not exactly independent of each other,[11] their interdependence can be ignored for all practically interesting situations. Therefore in what follows, we treat τ_1, ξ, and Λ as independent random variables.

Since the PMD vector attains the uniform distribution over the Poincaré sphere for transmission distances longer than a few kilometers, the two angles that characterize it, 2ξ and $\psi = \psi_1 + \psi_2$, have probability distributions $p(2\xi) = 1/2 \sin 2\xi$, $0 \leqslant 2\xi < \pi$, and $p(\psi) = 1/(2\pi)$, $0 \leqslant \psi < 2\pi$ (see, e.g., Ref. 12). That is, an average of any function $f(2\xi, \psi)$ is calculated as

$$\langle f(2\xi, \psi)\rangle = \frac{1}{4\pi}\int_0^{2\pi} d\psi \int_{2\xi=0}^{2\xi=\pi} d(2\xi) \sin 2\xi f(2\xi, \psi). \tag{10}$$

Therefore $\langle \cos^2 2\xi\rangle = 1/3$, $\langle \sin^2 2\xi\rangle = 2/3$. It was recently shown that the Stokes vector describing the transfer matrix T is also uniformly distributed on the Poincaré sphere,[13] and probability distributions of the angles 2φ and θ_1 satisfy $p(\varphi) = 1/2|\sin 2\varphi|$, $0 \leqslant \varphi < \pi$, and $p(\theta_1) = 1/\pi$, $0 \leqslant \theta_1 < \pi$. Then

$$\left\langle \frac{\sin^2(N\Lambda/2)}{\sin^2(\Lambda/2)} \right\rangle = \frac{1}{2\pi}\int_0^{\pi} d\theta_1 \int_0^{\pi} d\varphi \sin 2\varphi \times \frac{\sin^2(N \arccos[\cos\theta_1 \cos\varphi])}{\sin^2(\arccos[\cos\theta_1 \cos\varphi])}. \tag{11}$$

We have been unable to find a value for the above integral analytically and therefore evaluated it numerically for different N. The numeric value of the integral was always found to equal 1 within the accuracy of numerical integration; hence we concluded that

$$\left\langle \frac{\sin^2(N\Lambda/2)}{\sin^2(\Lambda/2)} \right\rangle = 1 \tag{11'}$$

for any integer N. Substituting this average value and the average values found immediately after Eq. (10) into Eq. (9), we obtain the main result of this paper:

$$\langle \tau_N^2\rangle = \langle \tau_1^2\rangle (N^2 + 2)/3. \tag{12}$$

The analytic formula (12) compares well with the results of a physical experiment that is presented in the next section.

3. EXPERIMENT

A. Background

We measure the DGD as a function of the number of round trips by means of a difference-frequency technique adapted to the conditions of a gated circulating loop. The instantaneous DGD is obtained by averaging the length of the arc described on the Poincaré sphere by the Stokes vectors at two frequencies $\omega_1 \approx \omega_2 \approx \omega$:

$$d\mathbf{S}/d\omega = \boldsymbol{\tau} \times \mathbf{S}. \tag{13}$$

Here $\mathbf{S}$ is the Stokes vector at the output of the system under test and $\boldsymbol{\tau}$ is the PMD vector, whose norm τ is the instantaneous DGD at frequency ω.[3] In this section, *all* quantities pertain to a given number N of circulations around the CL, and therefore we omit the subindex N used in Section 2. Instead, below we use the subindices $\{1, 2\}$ to denote the Stokes vectors pertaining to different frequencies ω_1 and ω_2. Equation (13) can be discretized using the midpoint rule of integration, resulting in

$$\|\mathbf{S}_2 - \mathbf{S}_1\|^2 = (\Delta\omega)^2 \tau^2 \left\| \frac{1}{2}(\mathbf{S}_1 + \mathbf{S}_2) \right\|^2 \sin^2\alpha, \tag{14}$$

where $\Delta\omega = (\omega_2 - \omega_1)$, $\|...\|$ denotes the norm of the vector, and α is the angle between $\boldsymbol{\tau}$ and $1/2(\mathbf{S}_1 + \mathbf{S}_2)$.

We note that the above discretization of Eq. (13) is strictly valid as long as $\Delta\omega\tau \ll \pi$ (Ref. 14) (note that other PMD measurement techniques impose similar requirements; see, e.g., Ref. 15). In our setup, $\Delta\omega \approx 2\pi \times 19$ GHz, which for the maximum DGD we measure yields $\Delta\omega\tau \approx 1.3$. Although the strong inequality $1.3 \ll \pi$ does not hold, the quantity $\Delta\omega\tau$ still turns out to be small enough to ensure that our results are consistent with the theory, as shown below. Taking the average of Eq. (14) and using the facts, pointed out in Section 2, that the DGD is not correlated to the angle of the PMD vector and that the output Stokes vector and the PMD vector are not correlated, we get

$$\sqrt{\langle \tau^2\rangle} = \frac{\sqrt{6}}{\Delta\omega}\left\langle \sqrt{\frac{\|\mathbf{S}_2 - \mathbf{S}_1\|^2}{\|\mathbf{S}_2 + \mathbf{S}_1\|^2}} \right\rangle. \tag{15}$$

In obtaining this equation, we have averaged over all possible polarization states of the system and used the relation $\langle \sin^2\alpha\rangle = 2/3$, which follows upon noticing that angles α and 2ξ in Section 2 have the same probability distributions. Thus the average DGD of the system around the optical frequency ω can be obtained from measurements of the Stokes vectors $\mathbf{S}_{1,2}$ at frequencies $\omega_{1,2}$ around ω.

B. Experimental Setup

Our setup is depicted in Fig. 1. The two wavelengths used for measuring the DGD are provided by two tunable lasers set at ω_1 and ω_2. These wavelengths are symmetric about one channel in the spectral grid defined by our interleavers; the corresponding channel as well as the two adjacent channels are turned off, leaving 61 channels at 100-GHz spacing running through the loop. These 61 support channels maintain the gain profile as used in transmission experiments. Each source can be turned on or off using an acousto-optic switch [AOS1 and AOS2 in

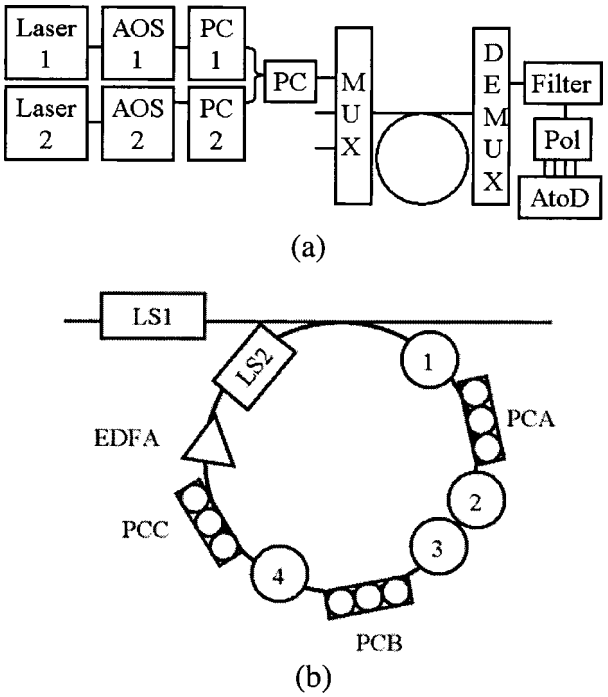

Fig. 1. Experimental setup: (a) General setup; AOS, acousto-optic switch; PC, manual polarization controller; HP-PC, HP8169 polarization controller; Mux, multiplexer; Demux, demultiplexer; Filter, 0.6-nm-wide spectral filter; HP-Pol, HP8509B polarimeter; AtoD, National Instruments PCI 1610 AtoD converter. (b) Close-up on the loop: LS1, load acousto-optic switch; LS2, loop acousto-optic switch; PCB and PCC, manual polarization controllers; PCA, voltage-controlled Polarite polarization controller.

Fig. 1(a)]. The signal paths are combined with a 3-dB coupler, and individual polarization controllers (PC1 and PC2) are used to align each signal to the input polarizer of an HP8169A polarization controller (HP-PC); the latter allows one to dial in the polarization state of the light that is injected into the loop. The output of the polarization controller is then combined with the 61 cw channels.

An AOS [LS1 in Fig. 1(b)] controls the loading of the signals into the circulating loop; the signals are loaded for the entire loop-transit time of 1.8 ms, and then blocked for 19.8 ms to accommodate 11 circulations. An intraloop AOS (LS2) is triggered with the inverse gating pattern to allow the signal to circulate around the loop. In this standard configuration, the signal (passing through LS1 or LS2) continuously flows from both output arms of the 3-dB coupler, into the receiver arm and into the first span. The loop is composed of four 80-km standard single-mode fiber (SSMF) Raman-pumped transmission spans. Each span is forward- and backward-Raman pumped, and is followed by a backward-pumped dispersion compensation module.[16] An erbium-doped fiber amplifier (EDFA) is used to overcome the loss of the intraloop AOS and 3-dB coupler. Intraloop polarization controllers (PCA, B and C) can be used to obtain the desired statistical measurement, as described in Subsections 3.D and 3.E below.

After the loop, the signal is filtered by means of a 100-to-200 GHz slicer and 0.6-nm optical filter centered between the frequencies under test. The state of polarization is measured by an HP8509B lightwave polarization analyzer. This polarimeter has four analog outputs that provide the degree of polarization and the three components of the Stokes vector of the light under test. These four outputs are sent to a National Instruments PCI 1610 analog-to-digital converter triggered by the load switch gating signal. A sampling rate of 100 kHz is sufficient to temporally resolve the Stokes vector during each round trip, as the loop round-trip time is 1.8 ms. An example of a measured component of the Stokes vector as a function of number of samples taken is shown in Fig. 2.

C. Temporally Resolved Stokes Vector

We first measured the Stokes vector at a fixed wavelength as a function of time. The AOS of one of the cw lasers was held in a passing state with the other blocking. All polarization controllers were fixed throughout this test. The Stokes vector, measured every 20 seconds over the total time of 1 hour and 20 minutes, is plotted in Fig. 3 for back-to-back operation (a), one (b), five (c), and ten (d) round trips. Note that for ten round trips (3200 km), the Stokes vector varies significantly (by about 20 degrees) over 20 seconds; thus accurately quantifying PMD requires a measurement technique that is much faster than this time interval. The output Stokes vector does not uniformly map the Poincaré sphere for any number of circulations, even during the measurement time of more than one hour. Therefore randomly tweaking the loop between each measurement of the DGD is necessary to average over all the polarization states of the loop. Another set of measurements performed every one second shows no significant change of the Stokes vector over 1 second, which justifies the averaging described in the next subsection to reduce noise.

D. Differential Group Delay in a Circulating Loop

The average DGD of the system was then measured. AOS1 and AOS2 were used to alternate between frequencies and every 21.6 ms (i.e., the loading plus transit time for 11 circulations). The Stokes vector for a given number of round trips was obtained by averaging over 50 data points within the associated 1.8-ms temporal window. Further averaging to reduce noise was performed over the Stokes vectors of 10 successive pairs of launches; each 432-ms ($10 \times 2 \times 21.6$ ms) averaging window constitutes a measurement over a single polarization state of

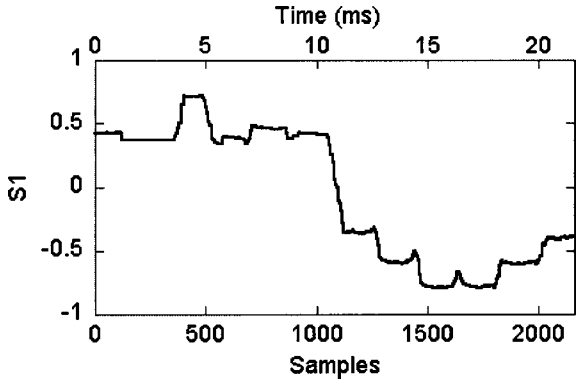

Fig. 2. Example of a time-resolved measurement of one coordinate of the Stokes vector. The lower scale corresponds to samples taken by the analog-to-digital board at a sampling rate of 100 kHz. The upper scale corresponds to time.

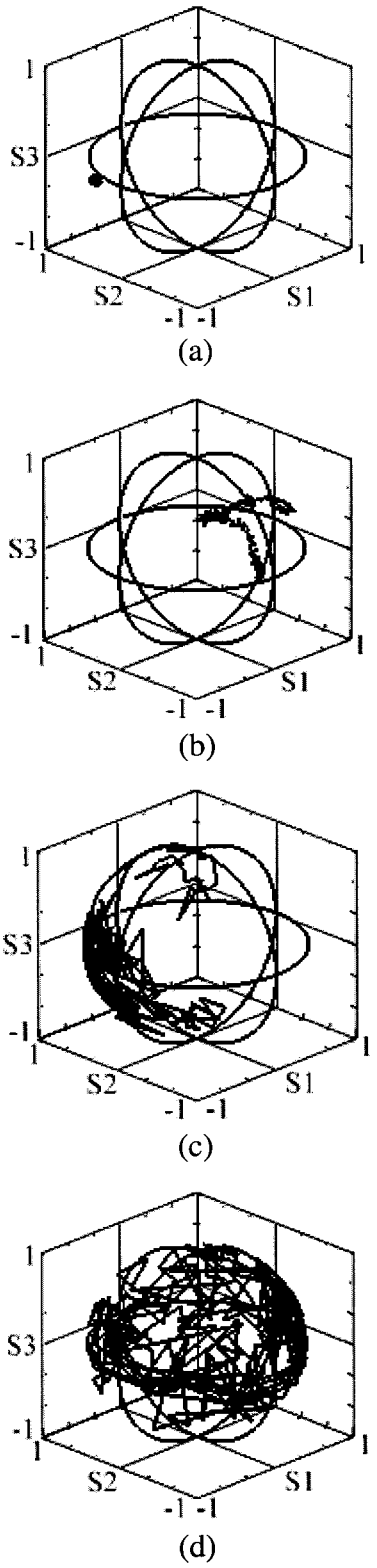

Fig. 3. Stokes vector on the Poincaré sphere at frequency measured every 20 seconds for (a) back-to-back, (b) one round trip, (c) five round trips, and (d) ten round trips. The measurement period was 1 hour and 20 minutes.

the loop. Proper averaging over the possible polarization states of the loop is ensured by manually tweaking the polarization controllers PCB and PCC [Fig. 1(b)] between each measurement of the DGD. The input Stokes vector was also randomly changed using the HP 8169A driven by a computer through a general purpose interface bus connection.

The DGD of the loop as a function of the number of circulations averaged over 100 measurements is plotted in Fig. 4 (triangular markers). It is close to linear, as expected from numerical simulations of Ref. 7 and the analytical formula (12) of Section 2. The solid curve is a fit using Eq. (12), which gives a value of the single-pass DGD $\sqrt{\langle \tau_1^2 \rangle} = 1.79$ ps, in reasonable agreement with the value of 1.5 ps obtained using the DGD of the individual standard single-mode fiber spans, dispersion compensation modules, in-loop EDFA, and gain-flattening filter while ignoring contributions from other in-loop components such as isolators and wavelength-division multiplexing couplers for Raman pumping. We also benchmarked measurements obtained with our technique against those obtained by a commercial, broadband PMD test set, using as a sample a one-meter length of polarization-maintaining fiber. For this case, our measurements yielded a three-percent larger value of DGD than that derived from the commercial set.

E. Differential Group Delay in a Randomized Loop

In order to obtain in a CL the square-root dependence of the mean DGD on the traveled distance, typical of straight-line systems, we have implemented an idea of Ref. 7 and randomized the polarization state of the signal at the beginning of each circulation around the CL, while not perturbing the PMD vector for a given round trip. This randomization is achieved by a General Photonics Polarite II low-loss polarization controller [PCA in Fig. 1(b)], which receives a set of 12 random voltage levels at the beginning of each load cycle; this set of 12 levels accommodates the 11 round trips plus initial loading time and is repeated for each load cycle. The measured average DGD as a function of the round-trip number for the randomized loop is plotted in Fig. 4 (square markers). The measurement can be fitted with a square root of the number of round trips as $\sqrt{\langle \tau_N^2 \rangle} \approx \sqrt{\langle \tau_1^2 \rangle}\sqrt{N}$, giving a single-pass average DGD of 1.53 ps, in good agreement with the value obtained for the nonscrambled loop and the value calculated from the independent measurement of the DGD of each element in the loop. Note that for a

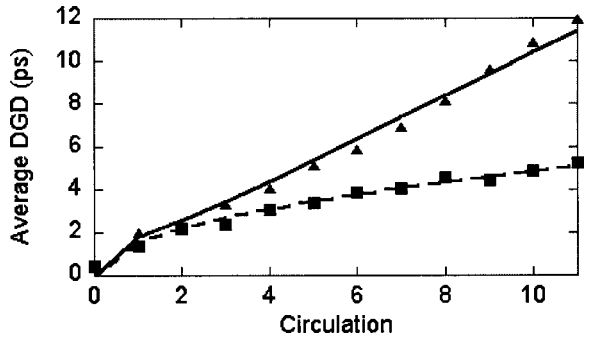

Fig. 4. Average DGD as a function of the number of circulations in the loop (triangular markers) and a fit using the analytic derivation (continuous line) for the nonscrambled loop; average DGD as a function of the number of circulations in the loop (square markers) and a fit using the analytic derivation (dotted curve) for the randomized loop.

large number of circulations, the average DGD of a randomized loop is significantly smaller than for the same physical loop without randomization.

4. DISCUSSION AND CONCLUSION

We begin this discussion by providing an intuitive explanation to the almost linear dependence of the mean DGD on the number of circulations, which follows from Eq. (12) and the experimental results of Section 3. Consider first a scalar counterpart of the PMD vector evolution. This is a Brownian motion, $\mathcal{B}$, driven by a source that is random in the interval $0 \leqslant z < L$ and repeats itself in each interval $nL \leqslant z < (n+1)L$, $n \geqslant 1$. If the standard deviation of $\mathcal{B}$ at $z = L$ equals σ_1, then, obviously, it equals $N\sigma_1$ at $z = NL$, where N is an integer. One may say that increments of $\mathcal{B}$ in each interval $nL \leqslant z < (n+1)L$ add up coherently. Now the magnitudes of the PMD vector increments acquired after each passage around the CL equal τ_1 (i.e., the DGD of a single passage). However, only *projections* of these increments onto, say, the direction of the PMD vector after the first passage, add coherently. The root-mean square value of such a projection is $\sqrt{\langle \cos^2 \phi_n \rangle} = 1/\sqrt{3}$, where ϕ_n is an angle between the PMD vector increments after the first and nth passages around the loop. Hence the magnitude of the total PMD vector after the Nth passage is $\sqrt{\langle \tau_N^2 \rangle} = \sqrt{\langle \tau_1^2 \rangle} \times N \times 1/\sqrt{3}$. This intuitively derived formula differs from the exact Eq. (12) by less than 5% when $N > 5$.

Another conclusion that can be drawn from Eq. (12) pertains to higher orders of PMD in a CL. Since the mean-square value of the mth order of PMD, $\langle |\boldsymbol{\tau}^{(m)}|^2 \rangle$, is proportional to $\langle \tau^2 \rangle^m$,[4] then in a CL, $\langle |\boldsymbol{\tau}^{(m)}|^2 \rangle$ accumulates with the number of passage as N^{2m}.

In conclusion, we have shown, both analytically and experimentally, that DGD of a circulating loop grows with the number of passages around the loop, or total transmission distance, approximately linearly; see Eq. (12) and Fig. 4. This dependence should be contrasted with the square-root dependence typical of straight-line transmission systems. We also experimentally verified the idea of Ref. 7, whereby by appropriate randomization of the signal's polarization at the beginning of each circulation around the CL, the average DGD was made to scale like the square-root of the number of circulations. These results are significant because of the utmost importance of circulating loops for the development of long-haul fiber-optic communication systems.

ACKNOWLEDGMENT

This work was completed when two of the authors (T. Lakoba and D. Maywar) were with Lucent Technologies, Holmdel, New Jersey. The authors thank the anonymous referee for his constructive comments.

*The author to whom all correspondence should be addressed.

REFERENCES

1. C. D. Poole and R. E. Wagner, "Phenomenological approach to polarization dispersion in long single-mode fibers," Electron. Lett. **22**, 1029–1030 (1986).
2. A. Caltarossa, A. Pizzinat, and F. Matera, "Statistical description of optical system performances due to random coupling on the principal states of polarization," IEEE Photon. Technol. Lett. **13**, 1307–1309 (2001).
3. M. Karlsson and J. Brentel, "Autocorrelation function of the polarization-mode dispersion vector," Opt. Lett. **24**, 939–941 (1999).
4. M. Shtaif and A. Mecozzi, "Mean-square magnitude of all orders of polarization mode dispersion and the relation with the bandwidth of the principal states," IEEE Photon. Technol. Lett. **12**, 53–55 (2000).
5. J. Garnier, J. Fatome, and G. Le Meur, "Statistical analysis of pulse propagation driven by polarization-mode dispersion," J. Opt. Soc. Am. B **19**, 1968–1977 (2002).
6. Q. Lin and G. P. Agrawal, "Correlation theory of polarization mode dispersion in optical fibers," J. Opt. Soc. Am. B **20**, 292–301 (2003).
7. S. Lee, Q. Yu, L.-S. Yan, Y. Xie, O. H. Adamczyk, and A. E. Willner, "A short recirculating fiber loop testbed with accurate reproduction of Maxwellian PMD statistics," *Optical Fiber Communication Conference*, Vol. 54 of OSA Trends in Optics and Photonics Series (Optical Society of America, Washington, D.C., 2001), paper WT-2.
8. H. Xu, J. Wen, J. Zweck, L. Yan, C. Menyuk, G. Carter, "The effects of distributed PMD, PDL, and loop scrambling on BER distributions in a recirculating loop used to emulate long-haul terrestrial transmission," *Optical Fiber Communication Conference*, Vol. 86 of OSA Trends in Optics and Photonics Series (Optical Society of America, Washington, D.C., 2003), paper TuO2.
9. H. Kogelnik, R. Jopson, and L. Nelson, "Polarization-mode dispersion," *Optical Fiber Telecommunications IV-B*, I. Kaminow and T. Li, eds. (Academic, New York, 2002), pp. 725–861.
10. J. P. Gordon and H. Kogelnik, "PMD fundamentals: polarization mode dispersion in optical fibers," Proc. Natl. Acad. Sci. **97**, 4541–4550 (2000).
11. Y. Tan, J. Yang, W. L. Kath, and C. R. Menyuk, "Transient evolution of the polarization dispersion vector's probability distribution," J. Opt. Soc. Am. B **19**, 992–1000 (2002).
12. S. V. Chernikov and J. R. Taylor, "Measurement of normalization factor of n_2 for random polarization in optical fibers," Opt. Lett. **21**, 1559–1561 (1996).
13. A. Vannucci and A. Bononi, "Statistical characterization of the Jones matrix of long fibers affected by polarization mode dispersion (PMD)," J. Lightwave Technol. **20**, 811–821 (2002).
14. B. L. Heffner, "Automated measurement of polarization mode dispersion using Jones matrix eigenanalysis," IEEE Photon. Technol. Lett. **4**, 1066–1069 (1992).
15. C. D. Poole and D. L. Favin, "Polarization-mode dispersion measurements based on transmission spectra through a polarizer," J. Lightwave Technol. **12**, 917–929 (1994).
16. D. N. Maywar, D. F. Grosz, A. Kung, L. Altman, M. Movassaghi, A. Agarwal, S. Banerjee, and T. H. Wood, "Ultrawideband transmission of 1.28 Tbit/s (128×10.7 Gbit/s) over 2000 km using 50% RZ data," Electron. Lett. **38**, 1573–1575 (2002).